

Supporting Information

MB₃P₂S₁₀ (M = Rb, Cs): Two New Alkali Metal Thioboratephosphates with [B₆P₄S₂₀] T3-Supertetrahedra

Jiazheng Zhou,^{‡a} Xin Su,^{‡c,d} Ling Luo,^e Junjie Li^{*b} and Feng Yu^{*a}

a. Key Laboratory for Green Processing of Chemical Engineering of Xinjiang Bingtuan, School of Chemistry and Chemical Engineering, Shihezi University, Shihezi, 832003, China;

b. Research Center for Crystal Materials; CAS Key Laboratory of Functional Materials and Devices for Special Environments, Xinjiang Technical Institute of Physics & Chemistry, CAS, Urumqi 830011, China;

c. School of Physical Science and Technology, Yili Normal University, Yining, 835000, China;

d. Xinjiang Laboratory of Phase Transitions and Microstructures of Condensed Matter Physics, Yili Normal University, Yining, 835000, China;

e. Department of Physics and Electronic Engineering, Xinjiang Key Laboratory for Luminescence Minerals and Optical Functional Materials, Xinjiang Normal University, Urumqi, 830054, China.

[‡]These authors contributed equally to this work.

*Corresponding authors (Email: yufeng05@mail.ipc.ac.cn; lijunjie@ms.xjb.ac.cn.)

Experimental Procedures

Reagents and Synthesis. All the raw reagents (RbCl/CsI, B, P, S) with high purities ($\geq 99.99\%$) were commercially purchased by Aladdin Industrial Inc. and were stored in a dry Ar-filled glovebox with limited oxygen and moisture levels below 0.1 ppm. The $\text{MB}_3\text{P}_2\text{S}_{10}$ (M = Rb, Cs) single crystals for structural determination were prepared by the flux method. The starting materials RbCl/CsI, B, P and S were weighed and loaded into graphite crucibles with the ratio of 1 : 3 : 2 : 10. The silica tubes were sealed with methane-oxygen flame under a high vacuum of 10^{-3} Pa. After that, the sealed tubes were put into a computer-controlled furnaces and heating program setting to $550\text{ }^\circ\text{C}$ in 20 h, kept at the temperature for 24 h, then the temperature was cooled to room temperature at a rate of $1\text{ }^\circ\text{C/h}$. Finally, the colorless single crystals for the title compound were harvest.

Single-Crystal X-ray Diffraction (XRD). High-quality transparent single crystals were selected under an optical microscope for collecting the X-ray diffraction data. A Bruker SMART APEX II CCD single crystal X-ray diffractometer using graphite-monochromatized molybdenum $K\alpha$ radiation ($\lambda = 0.71073\text{ \AA}$) was performed to collect the crystal data at room temperature. After collection, the SADABS program^[1] was used to perform the multiscan-type absorption correction of the structure data. After that, the XPREP program in the SHELXTL program package was used to determine the space group, and the SHELXT and XL programs were applied to solve and refine the structure data by direct methods and full-matrix least-squares on F^2 .^[2] Notably, during the structure refinements, a Q peak with a value of 1.58 was closed to the Rb atom. After the split operation, the values of R_1 and wR_2 were decreased from 5.91%, 15.48% to 4.17%, 11.30%, respectively, indicating the Rb atoms are disordered in the structure. Finally, the PLATON program was used to check the possible missing symmetry elements, and no higher symmetry was found.^[3]

Energy-Dispersive X-ray Spectroscopy (EDS). The EDS spectrum and mapping of the title compound were characterized on a field emission scanning electron microscope (FE-SEM, JEOL JSM-7610F Plus, Japan) equipped with an energy-dispersive X-ray spectrometer (Oxford, X-Max 50), which was operated at 5 kV. The energy-disperse X-ray spectroscopy (EDS) analyses were carried out on a single crystal of $\text{MB}_3\text{P}_2\text{S}_{10}$ (M = Rb, Cs). The EDS spectrum and mapping confirm the existence of Rb/Cs, P and S elements in the crystal

Raman Spectroscopy. $\text{MB}_3\text{P}_2\text{S}_{10}$ (M = Rb, Cs) crystals were put on a transparent glass slide, and then a LABRAM HR Evolution spectrometer equipped with a CCD detector by a 532 nm radiation was applied to investigate the Raman spectrum in the $4000\text{-}100\text{ cm}^{-1}$ region. The peaks around 665 cm^{-1} can be thought to A_1' vibrational modes of $[\text{BS}_4]$ units, the weak peaks around 783 cm^{-1} can be thought to T_2 vibrational modes of $[\text{BS}_4]$ units, The strong peaks around 220 cm^{-1} can be thought to the ν_2 and ν_4 modes result from the symmetric and asymmetric bending vibrations of the $[\text{PS}_4]$ units, The strong peaks around 440 cm^{-1} can be assigned to the ν_1 symmetric stretching mode within the $[\text{PS}_4]$ units, the weak vibrational around 548 cm^{-1} originates from the ν_3 asymmetric stretching of the $[\text{PS}_4]$ units, and the lowest wavenumbers around 50 to 154 cm^{-1} might be attributed to vibrations involving Rb^+ cations.

Theoretical Calculations. The band structure, total/partial density of states, and optical properties of $\text{MB}_3\text{P}_2\text{S}_{10}$ (M = Rb, Cs) were calculated by using the plane-wave pseudopotential method implemented in the CASTEP based on the density functional theory (DFT) method. Perdew-Burke-Ernzerhof (PBE) exchange-correlation of Generalized Gradient Approximation (GGA) was applied in the calculation. The interactions between core and electron were described by the norm-conserving pseudopotential (NCP)^[4]. The Monkhorst–Pack schemes was set as 0.05 \AA for $\text{RbB}_3\text{P}_2\text{S}_{10}$ and $\text{CsB}_3\text{P}_2\text{S}_{10}$. The valence electrons were set as Rb $4p^5 5s^1$, B $2s^2 2p^1$, P $3s^2 3p^3$ and S $3s^2 3p^4$ for $\text{RbB}_3\text{P}_2\text{S}_{10}$ and Cs $5p^5 6s^1$ B $2s^2 2p^1$, P $3s^2 3p^3$ and S $3s^2 3p^4$ for $\text{CsB}_3\text{P}_2\text{S}_{10}$. The kinetic energy cutoffs were set to be 650 eV . The Heyd-Scuseria-Ernzerhof 06 (HSE06) hybrid functional^[5] was performed using the PWmat code, which runs on graphics processing unit processors (GPU). The pseudo-potential NCPP-SG15-PBE pseudo-potential and 50 Ryd plane wave cut-off energy was used in the calculation.

$$E_{XC}^{HSE} = \alpha E_X^{HF,SR}(\mu) + (1 - \alpha) E_X^{PBE,SR}(\mu) + E_X^{PBE,LR}(\mu) + E_C^{PBE}$$

(α : mixing parameter; μ : adjustable parameter controlling the short-range of the interaction; $E_X^{HF,SR}(\mu)$: short range Hartree-Fock exact exchange functional; $E_X^{PBE,SR}(\mu)$ and $E_X^{PBE,LR}(\mu)$: short and long range components of the PBE exchange functional; E_C^{PBE} : PBE correlation functional) In HSE06, the parameters are suggested as $\alpha = 0.25$.

Table S1. Crystal data and structure refinements of Rb₂B₃P₂S₁₀ and Cs₂B₃P₂S₁₀.

Empirical formula	Rb ₂ B ₃ P ₂ S ₁₀	Cs ₂ B ₃ P ₂ S ₁₀
Formula weight (Da)	500.44	547.88
Temperature (K)	273.15	298.0
Crystal system, space group	tetragonal, <i>I</i> 4 ₁ / <i>a</i>	trigonal, <i>R</i> ³ <i>c</i>
Unit cell dimensions (Å)	<i>a</i> = <i>b</i> = 13.0688(13) <i>c</i> = 16.975(2)	<i>a</i> = <i>b</i> = 12.7539(8) <i>c</i> = 64.238(9)
Volume (Å ³)	2899.2(7)	9049.2(17)
<i>Z</i>	8	24
Calculated density (Mg/m ³)	2.293	2.413
Completeness (%)	100	100
Absorption coefficient (mm ⁻¹)	5.039	4.015
<i>F</i> (000)	6240	1936
2θ range for data collection/°	3.804 to 52.86	3.934 to 55.128
Index ranges	-15 ≤ <i>h</i> ≤ 15, -15 ≤ <i>k</i> ≤ 15, -80 ≤ <i>l</i> ≤ 80	-16 ≤ <i>h</i> ≤ 17, -16 ≤ <i>k</i> ≤ 16, -21 ≤ <i>l</i> ≤ 22
Reflections collected	41279	23060
Independent reflections	2072 [<i>R</i> _{int} = 0.0524, <i>R</i> _{sigma} = 0.0157]	1672 [<i>R</i> _{int} = 0.0743, <i>R</i> _{sigma} = 0.0340]
Observed reflections [<i>I</i> > 2σ(<i>I</i>)]	1992	1185
Data/restraints/parameters	2072/0/98	1672/0/85
Absorpt correction type	multi-scan	multi-scan
Goodness-of-fit on <i>F</i> ²	1.032	1.122
Final <i>R</i> indices (<i>F</i> _o ² > 2σ(<i>F</i> _o ²)) ^a	<i>R</i> ₁ = 0.0431, <i>wR</i> ₂ = 0.1027	<i>R</i> ₁ = 0.0302, <i>wR</i> ₂ = 0.0700
<i>R</i> indices (all data) ^a	<i>R</i> ₁ = 0.0657, <i>wR</i> ₂ = 0.1175	<i>R</i> ₁ = 0.0316, <i>wR</i> ₂ = 0.0710
Largest diff. peak and hole (e·Å ⁻³)	0.59 and -0.43	1.51 and -0.68

^a*R*₁ = Σ||*F*_o| - |*F*_c||/Σ|*F*_o| and *wR*₂ = [Σ*w*(*F*_o² - *F*_c²)/Σ*wF*_o⁴]^{1/2} for *F*_o² > 2σ(*F*_o²)

Table S2. Atomic coordinates, equivalent isotropic displacement parameters ($\text{\AA}^2 \times 10^3$) and BVS of $\text{Rb}_2\text{B}_3\text{P}_2\text{S}_{10}$.

Atoms	x	y	z	U_{eq}	Wyckoff positions	BVS ^[a]
Rb	0	1/2	1/2	119(3)	8 <i>d</i>	1.08 ^[b]
B1	1/4	1/4	0.5037(4)	38.2(14)	8 <i>e</i>	3.10
B2	0.4093(3)	0.3910(3)	0.3750(3)	36.2(10)	16 <i>f</i>	3.07
P1	0.26487(9)	0.30129(10)	0.50545(7)	46.3(3)	16 <i>f</i>	5.46
S1	0.60864(9)	0.22540(10)	0.57571(7)	50.6(3)	16 <i>f</i>	2.28
S2	0.52664(7)	0.37203(8)	0.44321(6)	35.0(2)	16 <i>f</i>	2.11
S3	0.42592(9)	0.51223(8)	0.31518(8)	47.1(3)	16 <i>f</i>	2.09
S4	0.29276(9)	0.42752(9)	0.43620(7)	45.4(3)	16 <i>f</i>	2.07

[a] The bond valence sum is calculated by bond-valence theory ($S = \exp[(R_0 - R)/B]$, where R is an empirical constant, R_0 is the length of bond I (in angstroms), and $B = 0.37$).

[b] For the split position, $S_{\text{Rb}} = S_{\text{Rb(A)}} \times a\% + S_{\text{Rb(B)}} \times b\%$ (where, a % and b % are the occupancies of Rb(A) and Rb(B).)

Table S3. Atomic coordinates, equivalent isotropic displacement parameters ($\text{\AA}^2 \times 10^3$) and BVS of $\text{Cs}_2\text{B}_3\text{P}_2\text{S}_{10}$.

Atoms	x	y	z	U_{eq}	Wyckoff positions	BVS ^[a]
Cs1	2/3	1/3	1/3	42.67(16)	6 <i>b</i>	1.10
Cs2	1/3	0.13456(3)	5/12	46.37(12)	18 <i>e</i>	1.03
B1	0.2311(3)	0.5072(3)	0.37096(6)	26.1(7)	36 <i>f</i>	3.05
B2	0.3892(3)	0.5634(3)	0.33177(5)	23.5(7)	36 <i>f</i>	3.06
P1	0.44768(8)	0.45544(8)	0.37121(2)	31.3(2)	36 <i>f</i>	5.41
P2	1/3	2/3	0.29135(2)	29.5(3)	12 <i>c</i>	5.43
S1	0.7121(8)	0.44059(8)	0.38175(2)	36.3(2)	36 <i>f</i>	2.14
S2	1/3	2/3	0.38263(2)	26.4(3)	12 <i>c</i>	2.19
S3	0.27400(8)	0.39460(8)	0.38219(2)	35.4(2)	36 <i>f</i>	1.99
S4	0.22410(6)	0.49826(6)	0.34102(2)	22.58(17)	36 <i>f</i>	2.23
S5	0.44473(8)	0.45477(7)	0.33909(2)	30.94(19)	36 <i>f</i>	2.11
S6	0.39393(8)	0.55391(8)	0.30217(2)	31.22(19)	36 <i>f</i>	2.12
S7	0.51274(9)	0.35464(9)	0.38059(2)	46.8(3)	36 <i>f</i>	2.05
S8	1/3	2/3	0.26100(2)	47.6(4)	12 <i>c</i>	1.97

[a] The bond valence sum is calculated by bond-valence theory ($S_{ij} = \exp[(R_0 - R)/B]$, where R is an empirical constant, R_0 is the length of bond I (in angstroms), and $B = 0.37$).

Table S4. Selected bond lengths of Rb₂B₃P₂S₁₀.

Atom	Atom	Length/Å	Atom	Atom	Length/Å
Rb1 ³	S1	3.5028(12)	Rb2	Rb2 ⁸	1.14(5)
Rb1	S5	3.2373(14)	B1	S1	1.901(4)
Rb1 ⁶	S5	3.4351(16)	B1	S2	1.929(4)
Rb2 ³	S1	3.704(19)	B2	S2	1.938(5)
Rb2 ⁴	S1	3.386(17)	B2 ¹	S2	1.934(5)
Rb2 ⁵	S3	3.46(2)	B2	S3	1.894(5)
Rb2	S4	3.729(19)	B2	S4	1.905(5)
Rb2 ⁶	S5	3.302(12)	P1 ²	S1	2.0681(17)
Rb2 ⁷	S5	3.653(12)	P1 ¹	S3	2.0609(19)
Rb2 ⁸	S5	3.416(18)	P1	S4	2.0580(17)
Rb2	S5	3.152(15)	P1	S5	1.9470(17)

¹1/4+Y,3/4-X,3/4-Z; ²1-X,1/2-Y,+Z; ³1/4+Y,1/4-X,1/4+Z; ⁴5/4-Y,1/4+X,5/4-Z; ⁵-1/4+Y,3/4-X,-1/4+Z; ⁶3/4-Y,1/4+X,1/4+Z; ⁷-1/4+Y,1/4-X,5/4-Z; ⁸-X,1-Y,1-Z

Table S5. Selected bond lengths of Cs₂B₃P₂S₁₀.

Atom	Atom	Length/Å	Atom	Atom	Length/Å
Cs1	S5 ¹	3.8641(8)	Cs2	S8 ¹⁰	3.7713(4)
Cs1	S5	3.8641(8)	Cs2	S8 ¹¹	3.7713(4)
Cs1	S5 ²	3.8640(8)	B1	S1	1.905(4)
Cs1	S5 ³	3.8641(8)	B1	S2	1.935(4)
Cs1	S5 ⁴	3.8641(8)	B1 ¹³	S2	1.935(4)
Cs1	S5 ⁵	3.8641(8)	B1 ¹²	S2	1.935(4)
Cs1	S7 ³	3.6987(12)	B1	S3	1.915(4)
Cs1	S7 ⁴	3.6986(12)	B1	S4	1.926(4)
Cs1	S7	3.6984(12)	B2	S4	1.930(3)
Cs1	S7 ⁵	3.6987(12)	B2 ¹²	S4	1.932(3)
Cs1	S7 ²	3.6987(11)	B2	S5	1.904(3)
Cs1	S7 ¹	3.6986(11)	B2	S6	1.909(4)
Cs2	S6 ⁵	3.7892(9)	S1 ¹³	P1	2.0729(13)
Cs2	S6 ⁶	3.7890(9)	S3	P1	2.0706(12)
Cs2	S1 ⁷	3.6520(9)	S7	P1	1.9419(12)
Cs2	S1 ⁸	3.6521(9)	P1	S5	2.0640(14)
Cs2	S7	3.4729(10)	P2	S6	2.0640(10)
Cs2	S7 ⁹	3.4729(10)	P2	S8	1.949(2)

¹1-Y,+X-Y,+Z; ²1/3+Y,2/3-X+Y,2/3-Z; ³4/3-X,2/3-Y,2/3-Z; ⁴1+Y-X,1-X,+Z; ⁵1/3-Y+X,-1/3+X,2/3-Z; ⁶1/3+Y-X,-1/3+Y,1/6+Z; ⁷+Y-X,-X,+Z; ⁸2/3-Y+X,1/3-Y,5/6-Z; ⁹2/3-X,1/3-X+Y,5/6-Z; ¹⁰1/3-X,2/3-Y,2/3-Z; ¹¹4/3-Y,2/3-X,1/6+Z; ¹²+Y-X,1-X,+Z; ¹³1-Y,1+X-Y,+Z

Table S6. Selected angles (°) of Rb₂B₃P₂S₁₀.

Atom	Atom	Atom	Angle/°	Atom	Atom	Atom	Angle/°
S1 ¹⁰	Rb1	S1 ¹¹	180	S5 ⁵	Rb2	S1 ¹¹	55.2(3)
S5 ¹²	Rb1	S1 ¹⁰	56.11(3)	S5	Rb2	S1 ¹⁰	100.1(4)
S5 ⁸	Rb1	S1 ¹⁰	83.95(4)	S5	Rb2	S1 ¹¹	81.9(4)
S5 ¹²	Rb1	S1 ¹¹	123.89(3)	S5	Rb2	S3 ⁷	91.6(6)
S5 ⁵	Rb1	S1 ¹¹	56.11(3)	S5 ⁸	Rb2	S3 ⁷	107.4(4)
S5	Rb1	S1 ¹⁰	96.05(4)	S5 ⁵	Rb2	S3 ⁷	88.7(4)
S5	Rb1	S1 ¹¹	83.95(4)	S5 ⁵	Rb2	S5 ⁸	63.1(3)
S5 ⁸	Rb1	S1 ¹¹	96.05(4)	S5	Rb2	S5 ⁸	160.6(7)
S5 ⁵	Rb1	S1 ¹⁰	123.89(3)	S5	Rb2	S5 ¹²	61.7(2)
S5 ⁸	Rb1	S5 ¹²	116.51(4)	S5 ⁸	Rb2	S5 ¹²	106.7(5)
S5	Rb1	S5 ¹²	63.49(4)	S5 ⁵	Rb2	S5 ¹²	162.1(8)
S5 ¹²	Rb1	S5 ⁵	180	S5	Rb2	S5 ⁵	123.1(5)
S5	Rb1	S5 ⁵	116.51(4)	S2	B1	S2 ²	115.6(3)
S5	Rb1	S5 ⁸	180	S1	B1	S2	110.33(6)
S5 ⁸	Rb1	S5 ⁵	63.49(4)	S1	B1	S2 ²	109.72(6)
S1 ¹⁰	Rb2	S4	129.2(7)	S1 ²	B1	S2	109.72(6)
S1 ¹¹	Rb2	S4	66.5(3)	S1 ²	B1	S2 ²	110.33(6)
S1 ¹⁰	Rb2	S1 ¹¹	162.2(7)	S1 ²	B1	S1	100.0(3)
S1 ¹⁰	Rb2	S3 ⁷	69.9(4)	S2 ⁶	B2	S2	115.2(2)
S1 ¹⁰	Rb2	S5 ¹²	55.1(2)	S4	B2	S2 ⁶	110.5(2)
S1 ¹⁰	Rb2	S5 ⁸	83.1(4)	S4	B2	S2	109.8(2)
S3 ⁷	Rb2	S4	67.1(4)	S3	B2	S2	109.7(2)
S3 ⁷	Rb2	S1 ¹¹	127.9(5)	S3	B2	S2 ⁶	110.5(2)
S3 ⁷	Rb2	S5 ¹²	108.9(5)	S3	B2	S4	100.1(2)
S5 ¹²	Rb2	S4	117.6(4)	S4	P1	S1 ²	108.85(8)
S5 ⁸	Rb2	S4	134.8(4)	S4	P1	S3 ⁶	109.60(8)
S5 ⁵	Rb2	S4	71.8(3)	S3 ⁶	P1	S1 ²	109.80(7)
S5	Rb2	S4	56.5(3)	S5	P1	S4	110.68(7)
S5 ⁵	Rb2	S1 ¹⁰	132.5(4)	S5	P1	S1 ²	108.73(8)
S5 ¹²	Rb2	S1 ¹¹	112.6(5)	S5	P1	S3 ⁶	109.18(8)
S5 ⁸	Rb2	S1 ¹¹	89.4(5)				

¹1/4+Y,3/4-X,3/4-Z; ²1-X,1/2-Y,+Z; ³1/4+Y,1/4-X,1/4+Z; ⁴5/4-Y,1/4+X,5/4-Z; ⁵-1/4+Y,3/4-X,-1/4+Z; ⁶3/4-Y,-1/4+X,3/4-Z; ⁷3/4-Y,1/4+X,1/4+Z; ⁸-X,1-Y,1-Z; ⁹-1/4+Y,1/4-X,5/4-Z; ¹⁰-1/4+Y,5/4-X,5/4-Z; ¹¹1/4-Y,-1/4+X,-1/4+Z; ¹²1/4-Y,1/4+X,5/4-Z

Table S7. Selected angles (°) of Cs₂B₃P₂S₁₀.

Atom	Atom	Atom	Angle/°	Atom	Atom	Atom	Angle/°
S5 ¹	Cs1	S5 ²	60.903(4)	S7 ⁴	Cs1	S7 ⁵	120.72(2)
S5 ³	Cs1	S5 ⁴	119.098(4)	S7 ²	Cs1	S7 ¹	120.72(2)
S5 ³	Cs1	S5	60.904(4)	S7 ²	Cs1	S7 ⁵	120.72(2)
S5 ¹	Cs1	S5 ⁵	119.097(5)	S7 ³	Cs1	S7 ¹	120.72(2)
S5 ²	Cs1	S5	180	S7 ³	Cs1	S7 ⁴	59.28(2)
S5 ¹	Cs1	S5 ³	60.902(5)	S7 ⁴	Cs1	S7 ¹	180
S5 ⁵	Cs1	S5 ⁴	60.903(4)	S7	Cs1	S7 ¹	59.29(2)
S5 ²	Cs1	S5 ³	119.095(4)	S7 ¹	Cs1	S7 ⁵	59.29(2)
S5 ¹	Cs1	S5	119.096(5)	S7 ³	Cs1	S7 ⁵	180
S5 ⁵	Cs1	S5 ³	180	S7 ²	Cs1	S7 ³	59.28(2)
S5 ⁵	Cs1	S5	119.097(5)	S7	Cs1	S7 ⁵	59.29(2)
S5 ¹	Cs1	S5 ⁴	180	S7 ²	Cs1	S7 ⁴	59.28(2)
S5 ⁴	Cs1	S5	60.905(5)	S7 ²	Cs1	S7	180
S5 ²	Cs1	S5 ⁴	119.096(5)	S6 ⁶	Cs2	S6 ³	177.68(3)
S5 ²	Cs1	S5 ⁵	60.903(5)	S1 ⁷	Cs2	S6 ⁶	61.54(2)
S7 ²	Cs1	S5 ¹	85.52(2)	S1 ⁸	Cs2	S6 ³	61.54(2)
S7	Cs1	S5	50.944(19)	S1 ⁸	Cs2	S6 ⁶	120.54(2)
S7 ²	Cs1	S5 ⁴	94.48(2)	S1 ⁷	Cs2	S6 ³	120.55(2)
S7 ³	Cs1	S5 ¹	71.55(2)	S1 ⁷	Cs2	S1 ⁸	77.20(3)
S7 ⁴	Cs1	S5 ³	94.48(2)	S1 ⁷	Cs2	S8 ⁹	95.37(2)
S7 ⁴	Cs1	S5 ¹	129.051(19)	S1 ⁷	Cs2	S8 ¹⁰	94.37(2)
S7 ¹	Cs1	S5 ⁴	129.056(19)	S1 ⁸	Cs2	S8 ⁹	94.36(2)
S7	Cs1	S5 ¹	94.48(2)	S1 ⁸	Cs2	S8 ¹⁰	95.37(2)
S7 ²	Cs1	S5 ³	108.45(2)	S7 ¹¹	Cs2	S6 ⁶	70.51(2)
S7 ¹	Cs1	S5 ¹	50.946(19)	S7 ¹¹	Cs2	S6 ³	108.32(3)
S7 ¹	Cs1	S5 ³	85.52(2)	S7	Cs2	S6 ⁶	108.32(3)
S7 ⁵	Cs1	S5 ¹	108.45(2)	S7	Cs2	S6 ³	70.50(2)
S7 ⁴	Cs1	S5 ⁴	50.947(19)	S7 ¹¹	Cs2	S1 ⁷	84.38(3)
S7 ²	Cs1	S5 ²	50.946(19)	S7 ¹¹	Cs2	S1 ⁸	147.81(2)
S7 ³	Cs1	S5	85.52(2)	S7	Cs2	S1 ⁷	147.81(2)
S7 ³	Cs1	S5 ²	94.48(2)	S7	Cs2	S1 ⁸	84.39(3)
S7 ⁵	Cs1	S5	94.48(2)	S7 ¹¹	Cs2	S7	122.79(4)
S7 ⁴	Cs1	S5 ²	108.45(2)	S7 ¹¹	Cs2	S8 ¹⁰	112.33(3)
S7 ³	Cs1	S5 ³	50.947(19)	S7	Cs2	S8 ⁹	112.33(3)
S7	Cs1	S5 ²	129.057(19)	S7 ¹¹	Cs2	S8 ⁹	61.06(3)
S7	Cs1	S5 ³	71.55(2)	S7	Cs2	S8 ¹⁰	61.06(3)
S7 ¹	Cs1	S5 ²	71.55(2)	S8 ⁹	Cs2	S6 ³	51.45(3)
S7 ⁵	Cs1	S5 ³	129.056(19)	S8 ⁹	Cs2	S6 ⁶	128.23(3)
S7 ⁵	Cs1	S5 ²	85.52(2)	S8 ¹⁰	Cs2	S6 ⁶	51.45(3)
S7 ³	Cs1	S5 ⁴	108.45(2)	S8 ¹⁰	Cs2	S6 ³	128.23(3)
S7 ²	Cs1	S5 ⁵	71.55(2)	S8 ⁹	Cs2	S8 ¹⁰	167.535(11)
S7	Cs1	S5 ⁴	85.52(2)	S4	B1	S2	115.85(17)
S7 ³	Cs1	S5 ⁵	129.051(19)	S1	B1	S4	109.20(18)
S7 ⁵	Cs1	S5 ⁴	71.55(2)	S1	B1	S2	109.66(18)
S7 ⁴	Cs1	S5 ⁵	85.52(2)	S1	B1	S3	99.90(16)
S7 ⁴	Cs1	S5	71.55(2)	S3	B1	S4	110.71(18)
S7	Cs1	S5 ⁵	108.45(2)	S3	B1	S2	110.33(18)
S7 ¹	Cs1	S5	108.45(2)	S4	B2	S4 ¹³	115.66(17)

S7 ¹	Cs1	S5 ⁵	94.48(2)	S6	B2	S4 ¹³	110.16(17)
S7 ⁵	Cs1	S5 ⁵	50.946(19)	S6	B2	S4	110.01(17)
S7 ²	Cs1	S5	129.053(19)	S5	B2	S4 ¹³	110.90(17)
S7 ⁴	Cs1	S7	120.72(2)	S5	B2	S4	109.46(16)
S7 ³	Cs1	S7	120.72(3)	S5	B2	S6	99.44(16)

¹1-Y,+X-Y,+Z; ²4/3-X,2/3-Y,2/3-Z; ³1/3-Y+X,-1/3+X,2/3-Z; ⁴1/3+Y,2/3-X+Y,2/3-Z; ⁵1+Y-X,1-X,+Z; ⁶1/3+Y-X,-1/3+Y,1/6+Z; ⁷2/3-Y+X,1/3-Y,5/6-Z; ⁸+Y-X,-X,+Z; ⁹1/3-X,2/3-Y,2/3-Z; ¹⁰4/3-Y,2/3-X,1/6+Z; ¹¹2/3-X,1/3-X+Y,5/6-Z; ¹²+Y-X,1-X,+Z; ¹³1-Y,1+X-Y,+Z; ¹⁴-Y,+X-Y,+Z; ¹⁵1/3-Y+X,2/3+X,2/3-Z

Table S8. Anisotropic displacement parameters ($\text{\AA}^2 \times 10^3$) for $\text{Rb}_2\text{B}_3\text{P}_2\text{S}_{10}$. The anisotropic displacement factor exponent takes the form: $-2\pi^2[h^2a^2U_{11}+2hka*b*U_{12}+\dots]$.

Atom	U_{11}	U_{22}	U_{33}	U_{23}	U_{13}	U_{12}
Rb1	166(9)	145(5)	46.3(13)	-19(3)	-35(4)	101(5)
Rb2	48(8)	59(5)	36(4)	0(2)	-13(3)	8(6)
B1	35(3)	45(4)	35(3)	0	0	12(3)
B2	30(2)	34(2)	44(3)	-0.2(19)	-3.2(19)	1.8(18)
P1	37.1(6)	51.0(7)	50.8(7)	5.8(6)	9.7(5)	11.6(5)
S1	46.8(7)	70.7(8)	34.4(6)	-2.5(5)	-7.4(5)	18.1(6)
S2	32.6(5)	36.3(5)	36.1(5)	-5.0(4)	-3.0(4)	4.2(4)
S3	45.9(6)	32.7(5)	62.7(8)	7.9(5)	-6.9(5)	0.1(4)
S4	37.8(6)	40.9(6)	57.6(7)	2.0(5)	2.8(5)	10.5(4)
S5	51.2(8)	75.7(10)	72.4(9)	16.8(7)	26.4(7)	22.6(7)

Table S9. Anisotropic displacement parameters ($\text{\AA}^2 \times 10^3$) for $\text{Cs}_2\text{B}_3\text{P}_2\text{S}_{10}$. The anisotropic displacement factor exponent takes the form: $-2\pi^2[h^2a^{*2}U_{11}+2hka^*b^*U_{12}+\dots]$.

Atom	U11	U22	U33	U23	U13	U12
Cs1	44.0(2)	44.0(2)	40.0(3)	0	0	22.01(11)
Cs2	54.4(2)	51.63(18)	34.0(2)	1.97(7)	3.94(15)	27.20(11)
S4	20.1(3)	18.8(3)	28.3(4)	-0.4(3)	1.0(3)	9.4(3)
S2	27.3(4)	27.3(4)	24.5(6)	0	0	13.7(2)
S6	37.4(4)	34.2(4)	27.3(4)	-2.5(3)	3.4(3)	21.9(4)
P2	33.1(5)	33.1(5)	22.4(7)	0	0	16.6(2)
S5	32.5(4)	28.3(4)	39.8(5)	2.6(3)	3.4(3)	21.1(3)
P1	29.2(4)	28.5(4)	40.3(5)	8.9(4)	0.6(4)	17.4(4)
S1	30.6(4)	32.3(4)	44.7(5)	12.3(4)	15.0(4)	14.8(4)
S3	33.7(4)	31.3(4)	43.8(5)	15.9(4)	8.8(4)	18.3(4)
S7	44.3(5)	47.8(5)	61.9(6)	24.0(5)	7.7(5)	33.3(5)
S8	60.5(7)	60.5(7)	21.7(8)	0	0	30.2(3)
B1	24.7(17)	22.9(17)	29.5(18)	6.4(14)	6.1(14)	10.9(14)
B2	22.6(16)	20.4(15)	28.7(18)	1.4(13)	1.2(13)	11.7(13)

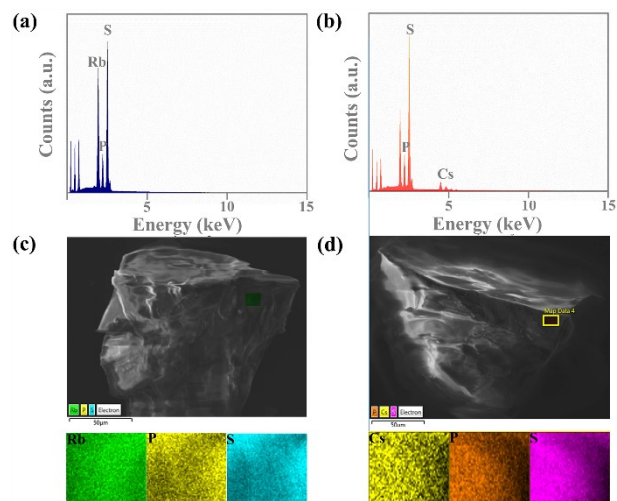


Figure S1. The EDS spectra, SEM images and mappings of $MB_3P_2S_{10}$ (M = Rb, Cs).

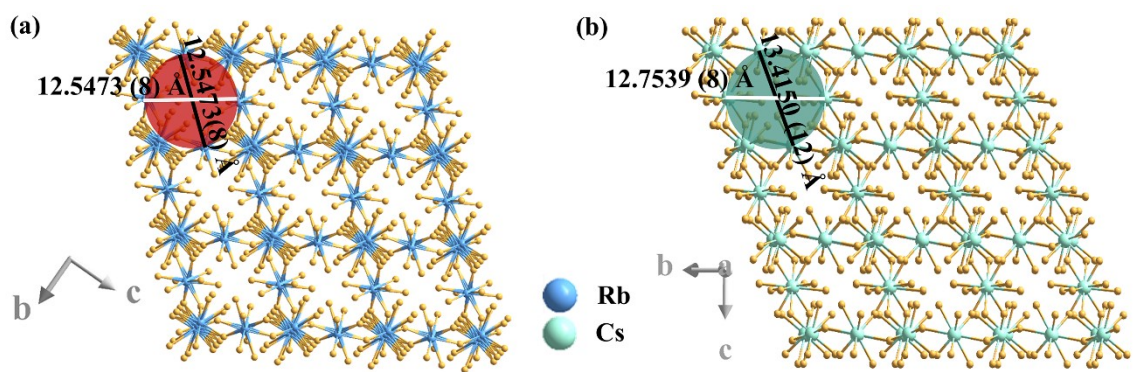


Fig. S2 The Rb-S 3D framework of $\text{RbB}_3\text{P}_2\text{S}_{10}$ (a) and the Cs-S 3D framework of $\text{CsB}_3\text{P}_2\text{S}_{10}$ (b) viewed along a direction.

References

- [1] L. Haeming, G. M. Sheldrick, SADABS: A Program for Exploiting the Redundancy of Area-Detector X-Ray Data. *Acta Crystallogr. A* **1999**, *55*, 206-206.
- [2] G. M. Sheldrick, A Short History of SHELX. *Acta Crystallogr. A* **2008**, *64*, 112-122.
- [3] A. L. Spek, Single-crystal Structure Validation with the Program PLATON. *J. Appl. Crystallogr.* **2003**, *36*, 7-13.
- [4] a) J. P. Perdew, K. Burke, M. Ernzerhof, Generalized Gradient Approximation Made Simple. *Phys. Rev. Lett.* **1997**, *78*, 1396-1396; b) A. M. Rappe, K. M. Rabe, E. Kaxiras, J. D. Joannopoulos, Optimized Pseudopotentials. *Phys. Rev. B* **1990**, *41*, 1227-1230; c) D. Vanderbilt, Soft Self-Consistent Pseudopotentials in a generalized Eigenvalue Formalism. *Phys. Rev. B* **1990**, *41*, 7892-7895; **2006**, *125*, 224106; d) S. J. Clark, M. D. Segall, C. J. Pickard, P. J. Hasnip, M. J. Probert, K. Refson, M. C. Payne, First Principles Methods Using CASTEP. *Z. Kristallogr.* **2005**, *220*, 567-570.
- [5] a) J. Heyd, J. E. Peralta, G. E. Scuseria, R. L. Martin, Energy Band Gaps and Lattice Parameters Evaluated with the Heyd-Scuseria-Ernzerhof Screened Hybrid Functional. *J. Chem. Phys.* **2005**, *123*, 224106. b) A. V. Krukau, O. A. Vydrov, A. F. Izmaylov, G. E. Scuseria, Influence of the Exchange Screening Parameter on the Performance of Screened Hybrid Functionals. c) J. Heyd, G. E. Scuseria, M. Ernzerhof, Hybrid Functionals Based on a Screened Coulomb Potential. *J. Chem. Phys.* **2003**, *118*, 8207-8215.